J Solid State Electrochem (2012) 16:1415–1421
DOI 10.1007/s10008-011-1541-2

ORIGINAL PAPER

Multi-wall carbon nanotube counter electrodes for dye-sensitized solar cells prepared by electrophoretic deposition

Jeng-Yu Lin · Chih-Heng Lien · Shu-Wei Chou

Received: 25 July 2011 / Revised: 15 August 2011 / Accepted: 23 August 2011 / Published online: 8 September 2011

Abstract In this study, electrophoretic deposition (EPD) was employed to fabricate multi-wall carbon nanotube (MWCNT) counter electrodes (CEs) for dye-sensitized solar cells (DSSCs). Firstly, raw MWCNTs were functionalized by means of an acid mixture solution and then subjected to EPD. The results obtained from Raman spectroscopy, Fourier transform infrared spectroscopy, field-emission scanning electron microscope, and cyclic voltammogram demonstrated that the defects and open ends on the MWCNTs can be obtained via chemical functionalization and thus facilitate the enhancement in the electrocatalytic activity for I_3^- reduction of MWCNT CEs. In addition to optimizing chemical functionalization of MWCNTs surface, the optimal thickness of MWCNT CEs prepared by EPD was also investigated. Additionally, consecutive cyclic voltammetric tests demonstrated that the MWCNT CE fabricated by EPD possessed excellent electrochemical stability. In comparison with MWCNT CEs fabricated by tape-casting approach, MWCNT CEs prepared by EPD presented a superior adhesion between MWCNT deposits and conducting glass substrates. Therefore, MWCNT CEs fabricated by EPD can be of great potential for use in low-cost plastic DSSCs.

J.-Y. Lin (✉) · S.-W. Chou
Department of Chemical Engineering, Tatung University,
Taipei 104, Taiwan
e-mail: jylin@ttu.edu.tw

C.-H. Lien
Department of Chemical Engineering,
National Tsing-Hua University,
Hsinchu 300, Taiwan

Keywords Multi-wall carbon nanotube · Electrophoretic deposition · Electrocatalytic activity · Counter electrode · Dye-sensitized solar cell

Introduction

In recent years, dye-sensitized solar cells (DSSCs) have aroused intensive interests as a low-cost alternative to conventional inorganic p–n junction photovoltaic devices [1]. In order to further reduce the cost of DSSCs, the ways in finding cheaper raw materials and simplifying the fabrication procedure have been extensively considered. In a DSSC, counter electrode (CE) plays an important and indispensable role in collecting electrons from external circuit and reducing I_3^- to I^- for the regeneration of sensitizer after electron injection. The noble metal Pt is widely used as a CE due to its superior electrocatalytic activity, excellent electrochemical and chemical stability, as well as high conductivity. Although the necessary amount of Pt as an effective CE material is very low, ca. 10–100 μg cm^{-2} [2, 3], a great deal of research has been dedicated to the development of alternatives capable of Pt CE using carbonaceous materials, such as graphite, activated carbon, carbon black and carbon nanotubes (CNT) [4–11], conducting polymer [12–15], and CoS CEs [16–19] in view of the limited resources and expensive price of Pt.

Among the carbonaceous materials, the fast electron transfer kinetics and the large surface area of CNTs have attracted considerable interest for use as a CE in DSSCs [20, 21]. Until now, various approaches have been developed to fabricate CNT CEs, such as screen printing [10], spray dry [6], doctor blade [8], and chemical vapor deposition [11]. Most of the methods require a high temperature treatment to remove the binder from the paste

after the coating. Although Mei et al. [22] proposed a binder-free method to fabricate MWCNT CEs for high-performance DSSCs, two-step high temperature treatments were still used in their study. The use of heat treatment excludes the choice of flexible plastic substrates, and thus the development of low temperature methods to fabricate the CNT CEs is needed for flexible DSSCs.

In this study, electrophoretic deposition (EPD) was employed to fabricate multi-wall carbon nanotube (MWCNT) CEs for DSSCs at low temperature and to explore methods for increasing their electrocatalytic activity through film processing including chemical functionalization degree and thickness of MWCNT deposits by means of Raman spectra, field-emission scanning electron microscopy (FESEM), and cyclic voltammetry (CV) analyses. Moreover, the adhesion and electrocatalytic ability of the MWCNT CE fabricated by the EPD were in comparison with those of the MWCNT CE prepared by a tape-casting processing in this study.

Experimental

Raw MWCNTs (Golden Innovation Business Co.) were refluxed in a 3:1 mixture of 98% H_2SO_4 and 78% HNO_3 at 120 °C for a fixed time to functionalize the graphitic sp^2 carbon into a –COOH functional group on the side walls of the MWCNTs. The functionalized MWCNTs were further filtered by suction filtration, washed thoroughly with deionized water, and subjected to drying. The resulting functionalized MWCNTs were suspended in a 1:1 mixture of acetone and ethanol by ultrasonication for 2 h. The aqueous MWCNT suspensions of 5 mg mL^{-1} concentrations were used for the electrophoresis experiments. Cleaned fluorinated tin oxide (FTO) glass substrates (NSG, 13 Ω/sq) with a dimension of 15×20×2.2 mm and a Pt sheet (2 cm^2) were used as a working electrode and a counter electrode, respectively. These two electrodes were positioned in parallel with a distance of 0.7 cm apart from each other. A constant potential of 18 V vs. open-circuit potential was employed for the EPD. Subsequently, the resulting MWCNT CEs were dried at 50 °C for 5 min. For comparison, a MWCNT CE fabricated by tape-casting processing was also made in this study. The MWCNT paste for the tape-casting processing was composed of MWCNTs, an organic binder, and distilled water [10]. A total of 0.16 g of (carboxymethyl)-cellulose sodium salt was dissolved in 19.84 mL of distilled water. A total of 1.13 g CNTs was then added to the binder solution and then sonicated for 1 h. The resulting homogeneous MWCNTs slurry was tape-casted onto a previously cleaned FTO glass substrate followed by drying at 50 °C for 10 h in air.

The TiO_2 photoanodes were fabricated on the cleaned FTO by screen printing technique. A 12-μm-thick layer as an interlayer was first printed on the FTO glass substrate and further coated by 2-μm-thick light-scattering anatase TiO_2 particles (Tripod Technology Co.). The detailed fabrication procedure and composition of the TiO_2 pastes for screen printing was described elsewhere [23]. After screen printing, the as-prepared TiO_2 photoanodes were heated at 450 °C for 2 h. When the temperature of the pre-heated photoanodes was cooled down to 40 °C, they were dipped into an ethanol solution containing 0.3 mM N719 dye (Everlight Chemical Industry Co.) for 4 h. The sensitized TiO_2 photoanodes were rinsed with ethanol and then subjected to be dried under a cool air flow. The TiO_2 photoanodes and various CEs were sealed with a thermoplastic hot-melt surlyn (30 μm in thickness, Dupont), and the electrolyte composed of 1 M 1, 3-dimethylimidazoliumiodine, 0.5 M 4-tert-butylpyridine, 0.15 M iodine, and 0.1 M guanidine thiocyanate in 3-methoxypropionitrile was injected into the cell through the pre-drilled holes, which were further sealed after electrolyte injection .

The carboxy groups on MWCNTs surface were analyzed by Fourier transform infrared spectroscopy (FTIR) before and after chemical functionalization. The degree of chemical functionalization for MWCNTs was further evaluated using Raman spectroscopy. The surface morphology of MWCNT CEs was characterized by means of a FESEM (JSM-7000F). The CV measurements were conducted using a 4-cm^2 Pt sheet as auxiliary electrode, a Pt wire as reference electrode, and the as-prepared MWCNT CEs as the working electrode with a total exposure area of 0.64 cm^2 in a 3-methoxypropionitrile solution consisting of 50 mM LiI, 10 mM I_2, and 500 mM $LiClO_4$. The scan rate was set at 10 mV s^{-1} and data were acquired in the potential interval ranging from −1.2 V to 1.2 V vs. Pt using a potentiostat (Solartron). The photocurrent density–voltage (*I–V*) characteristic was carried out using a computer-controlled Keithley 2400 source meter under illumination by a solar simulator (Yamashita Denso YSS-150A). The active cell area and the incident light intensity were controlled at 0.28 cm^2 and 100 mW cm^{-2} (AM 1.5), respectively.

Results and discussion

Figure 1 shows the FESEM images of MWCNTs before and after in the refluxed acid mixture solution. The MWCNTs after refluxing in the acid mixture for 60, 90, and 120 min were called MWCNT-A, MWCNT-B, and MWCNT-C, respectively. It can be observed that the diameter and length of MWCNTs slightly decreased and became shorter with increasing reflux interval, respectively,

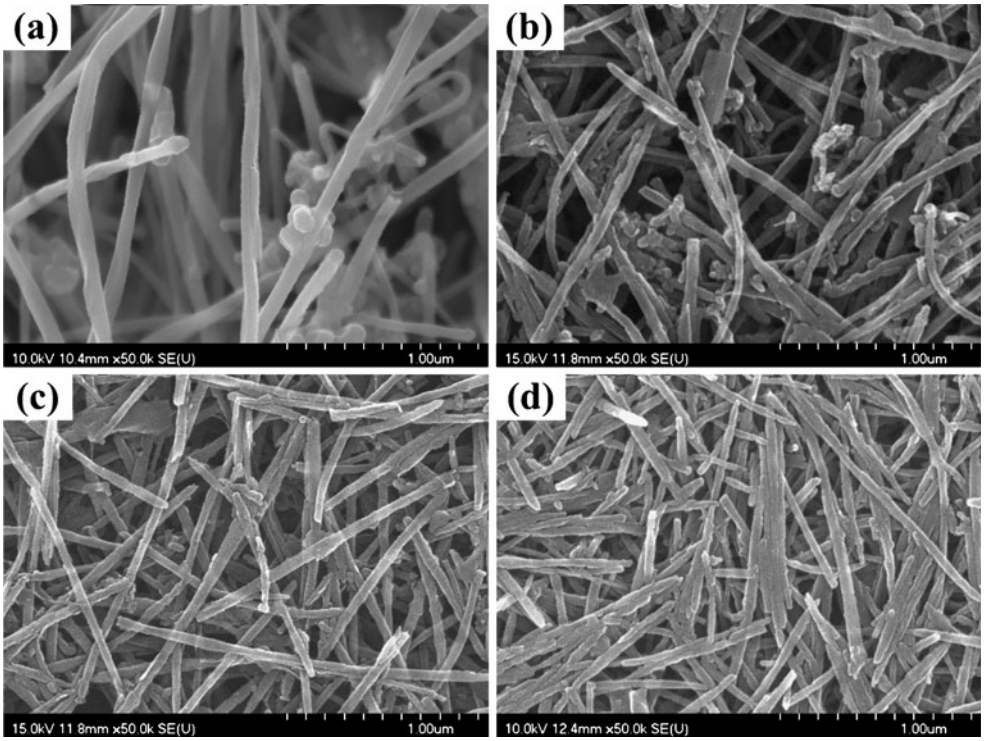

Fig. 1 Top view FESEM images of **a** raw MWCNT, **b** MWCNT-A, **c** MWCNT-B, and **d** MWCNT-C on FTO glass substrates

especially on MWCNT-C. Chiang et al. [24] proposed a successive and iterative process for MWCNTs in H_2SO_4/HNO_3 mixture, including the initial attack on active sites and next the hexagon electrophilic attacks to generate new defects and introduce more oxygen, thus resulting in the MWCNTs becoming thinner and shorter. Consequently, the fracture of MWCNTs can be attributed to chemical functionalization. Chemical functionalization could generate the defect- and disorder-induced modes in the MWCNTs, thus increasing the intensity of the D peak, a phonon mode at 1,350 cm^{-1} in Raman spectra. The degree of functionalization of MWCNT surface can be evaluated by comparing the intensity of D band and G band ratio (I_D/I_G) of MWCNTs after chemical functionalization. Consequently, Raman spectroscopy was conducted to evaluate the functionalization degree for MWCNT films treated in different reflux times, as shown in Fig. 2. The values of I_D/I_G ratio for each functionalized MWCNT films are also listed in Fig. 2. It can be found that the D band and G band can be clearly observed at ~1,350 and 1,580 cm^{-1} for all MWCNTs. The increase in I_D/I_G ratio of MWCNTs can be found with increasing the reflux time, indicating that the density of defects on MWCNTs increased and the conductivity decreased. It should be noted that the highest I_D/I_G ratio of 0.408±0.035 can be obtained in the case of MWCNT-C. This indicates that the degree of functionalization on the surface of MWCNTs can be controlled by reflux time in the acid mixture solution.

The functional groups attached to the functionalized MWCNTs were analyzed by means of FTIR spectroscopy. Figure 3 presents the FTIR spectra of raw MWCNT and functionalized MWCNTs. In Fig. 3a, the main absorption bands were assigned as follows: the carbon–carbon single bond (C–C) sketching vibrations at 1,581 cm^{-1}, the carbon–carbon double bond (C=C) stretching at 1,719 cm^{-1}, and alky CH_x stretching at 2,850–2,950 cm^{-1}. The appearance of O–H bond in the raw MWCNTs represents that there was some water absorption on the surface of raw MWCNTs. In comparison with Fig. 3a, the absorption peaks of carbon–

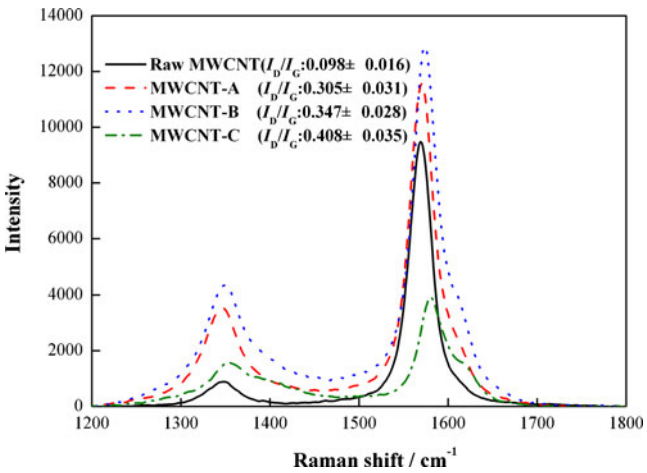

Fig. 2 Raman spectrum of various MWCNTs

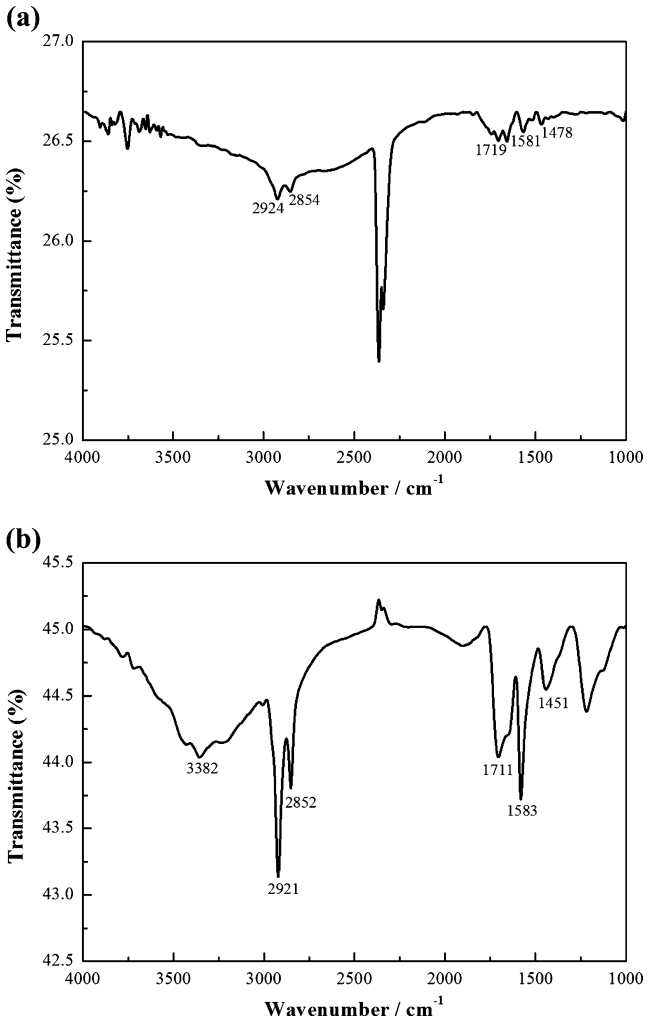

Fig. 3 FTIR spectrum of **a** raw MWCNT and **b** MWCNT-C

oxygen double bond (C=O) and the oxygen–hydrogen single bond (O–H) stretching at 1,711 and 3,382 cm^{-1} were found on the surface of functionalized MWCNT-C, respectively, as shown in Fig. 3b. This clearly indicates the formation of a carboxylic group (–COOH) on the surface of functionalized MWCNT-C.

Figure 4a presents the CV of MWCNT CEs with various reflux times. The electrophoretic deposition was not successfully carried out for the unmodified MWCNTs due to the lack of a carboxylic function group. Thus, the raw MWCNT CE prepared by electrophoretic deposition was not considered in Fig. 4. The relationship between the resulting cathodic peak current densities and potentials and the reflux time for various MWCNT CEs are also illustrated in Fig. 4b. The increase in cathodic peak current density and the decrease in cathodic potential with increasing the degree of functionalization of the MWCNT surface can be noted. Banks et al. [25] found that the graphite surface with a large quantity of edge plane can provide faster electron transfer compared to that with the basal plane. They also reported that the electrocatalytic response of an edge plane on the graphite electrode surface was similar to that of a MWCNT. Thus, the surface defects formed after chemical functionalization can act as the edge plane at a graphite surface. It can be suspected that more edge planes can be formed on the MWCNT surface while the degree of functionalization on the MWCNT surface increases, thus resulting in the enhancement in electron transfer from MWCNTs to electrolyte. Moreover, it can be observed that MWCNTs tended to break when refluxing in acid mixture solution (especially on MWCNT-C), and thus more open ends of MWCNTs can be formed. The open ends of MWCNTs can provide active sites for electrocatalytic reaction, thus enhancing the electrocatalytic activity of MWCNT films. Consequently, MWCNT-C with highest electrocatalytic activity for reduction of I_3^- to I^- can be obtained. The *I–V* measurements of DSSCs with MWCNTs in different reflux times were conducted and illustrated in Fig. 5. It can be observed that both of the short-circuit photocurrent (J_{sc}) and open-circuit voltage (V_{oc}) increased

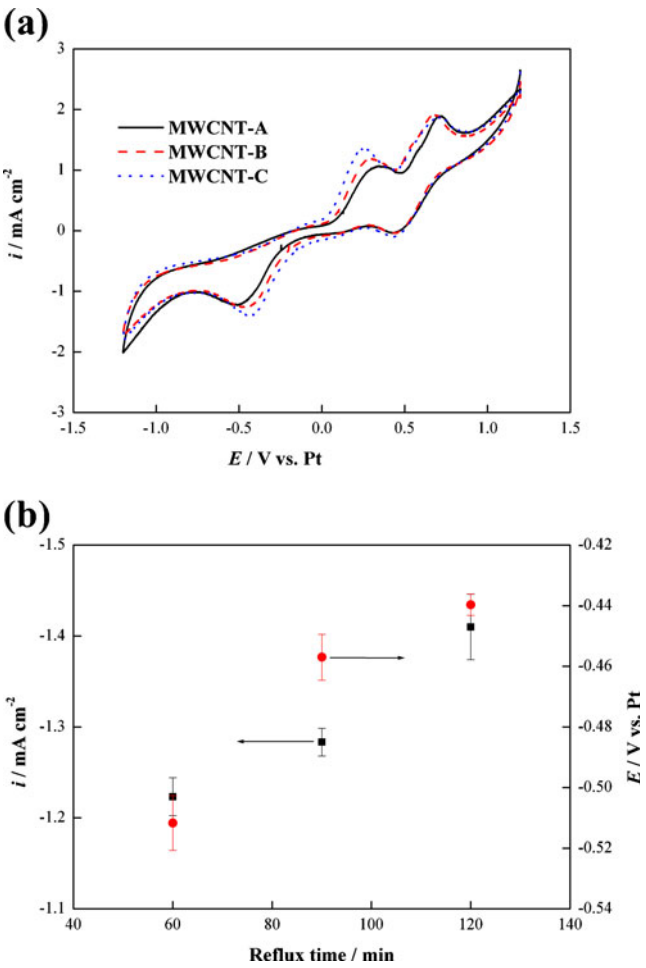

Fig. 4 **a** CV of MWCNT-A, MWCNT-B, and MWCNT-C CEs at a scan rate of 10 mV s^{-1}. **b** The relationship between reflux times and the cathodic peak currents and potentials. The thickness of the MWCNT CEs was controlled at ~6 μm

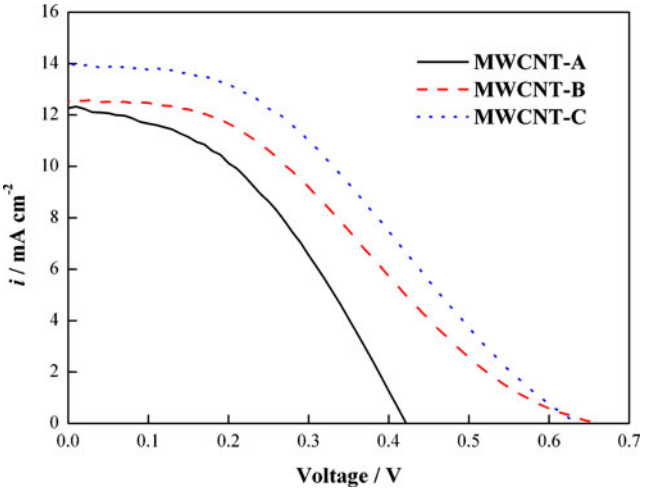

Fig. 5 Photocurrent density–voltage characteristics of MWCNT-A, MWCNT-B, and MWCNT-C

with increasing the reflux time; thus, enhanced conversion efficiency of DSSCs assembled with MWCNT CEs can be obtained from 2.16% (MWCNT-A) to 3.32% (MWCNT-C) by controlling the functionalization degree of MWCNTs surface. This is in accordance with the observation from CV measurements.

Furthermore, the electrocatalytic activity of MWCNT-C with different thickness values was investigated, as shown in Fig. 6a. The relationship between the resulting cathodic peak current densities and potentials of MWCNT-C CEs with different thickness values are also presented in Fig. 6b. The cathodic peak current density increased and the cathodic potential decreased with the increase in the thickness of MWCNT-C CEs, indicating that the electrocatalytic activity of MWCNT-C CE can be further enhanced by increasing the thickness. With the consecutive 50-cycle test, the CV did not change but exhibited stable anodic and cathodic peak current densities as shown in Fig. 6c. This indicates that the MWCNT-C CE did not only possess good electrochemical stability but was also attached firmly and uniformly on the FTO substrate.

To further find out the optimal thickness of MWCNT-C CEs, *I–V* measurements of DSSCs with MWCNT-C CEs in different thickness values were carried out. Figure 7 summarizes the relationship between the resulting photovoltaic parameters obtained from *I–V* curves and the thickness of MWCNT-C CEs. The value of J_{sc} is almost similar with the increasing thickness of MWCNT-C CE. One interesting result lies in the decrease in V_{oc} with increasing the thickness of MWCNT-C CEs, thus resulting in such a way that the cell efficiency of DSSCs assembled with MWCNT-C CEs initially increased and then decreased with increasing the thickness of MWCNT-C CEs. Since the effect of the thickness on V_{oc} and *FF* was observed in the opposite tendency, there was an optimum thickness of MWCNT-C CE based on the aforementioned results. The highest efficiency was obtained when the thickness of MWCNT-C CE was controlled at ~4 to 5 μm. According to the previous study reported by Murakami et al. [9], two possible explanations can be proposed: one is adsorption of electrolyte, like 4-tert-

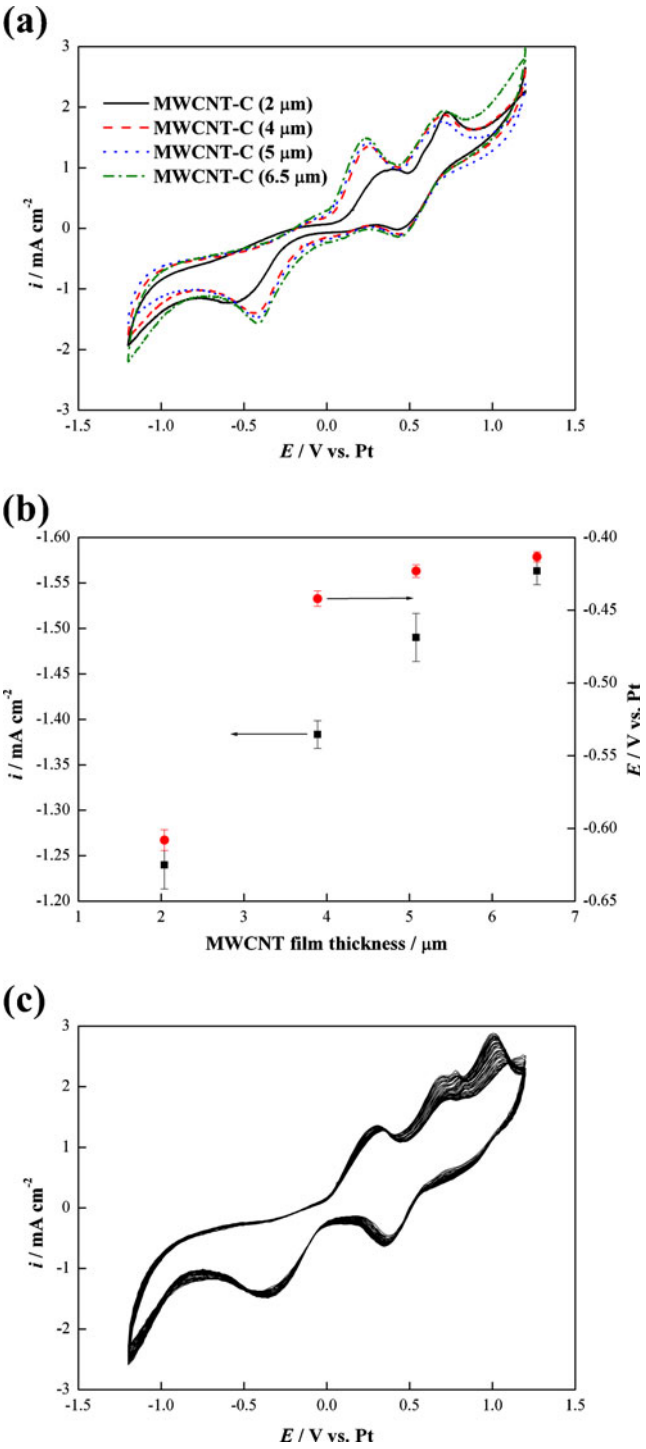

Fig. 6 **a** CV of MWCNT-C CEs with various thicknesses at a scan rate of 10 mV s^{-1}. **b** The relationship between film thicknesses and the cathodic peak currents and potentials. **c** Consecutive 50 CV of I^-/I_3^- for MWCNT-C CE

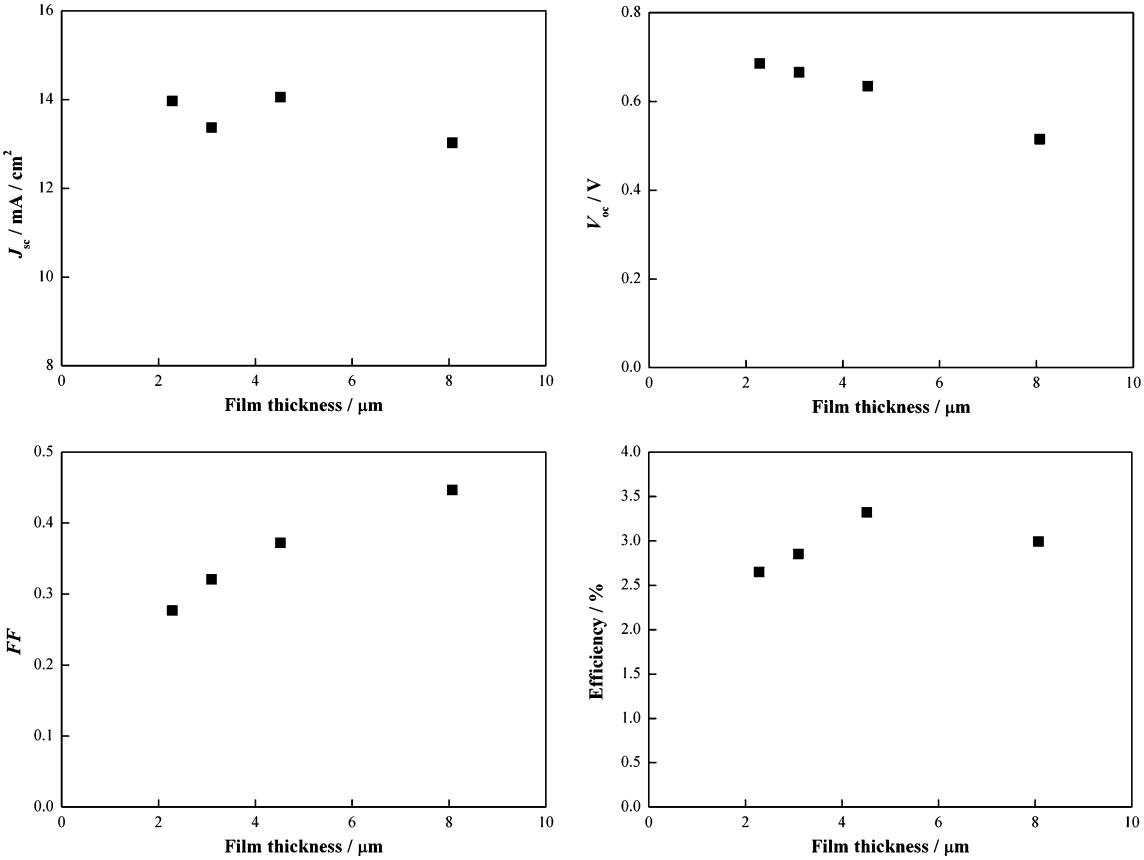

Fig. 7 Variations of photovoltaic parameters with film thickness for the DSSC with the MWCNT-C CEs

butylpyridine onto the carbon surfaces; the other one is localized short circuiting between TiO_2 layer and MWCNT film. Depositing the thick MWCNT film can provide more surface area, thus improving the electrocatalytic activity for reduction of I_3^- to I^- and *FF*. It could lead to obtaining a lower V_{oc} and thus lowering the cell performance of DSSCs.

To further ascertain if the EPD is a feasible method to fabricate NWCNT CEs, the MWCNT-C CE fabricated by the EPD was compared with that prepared by the tape-casting approach. The as-prepared MWCNT-C CEs were subjected to the scotch tape test to evaluate the interface adhesion between MWCNT-C film and FTO glass substrate, as shown in Fig. 8. After the tape test, less amount of MWCNT-C was detached from the CNT electrode by EPD compared to that by tape-casting method. This indicates that the adhesion between MWCNT-C film and FTO glass substrate can be enhanced by EPD approach. Moreover, CV

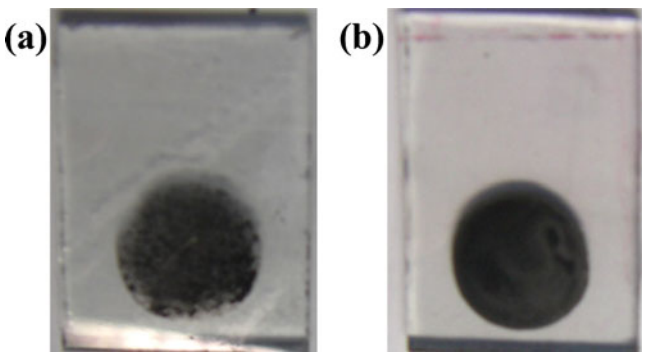

Fig. 8 Images of MWCNT electrodes prepared by **a** tape-casting and **b** EPD after Scotch tape tests

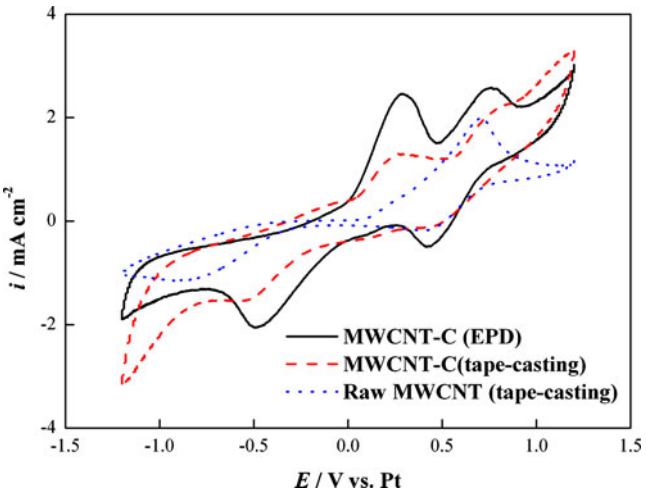

Fig. 9 CV of raw MWCNT and MWCNT-C CEs prepared by tape-casting method, and MWCNT-C CE fabricated by EPD. The thickness of all MWCNT CEs was controlled at ~17.5 μm

was carried out and shown in Fig. 9 to compare the electrocatalytic activity of raw MWCNT and MWCNT-C CEs by tape-casting and EPD, respectively. Obviously, the electrocatalytic activity of MWCNT-C CE by EPD was better than that by tape-casting method. The MWCNT-C electrode fabricated by tape-casting method had lower peak current density and higher overpotential probably due to the use of binder in the paste for coating MWCNT-C film on the FTO glass substrate. It may result in some shielding effect on MWCNT-C, thus lowering its electrocatalytic activity. In addition to comparing with MWCNT-C CE fabricated by EPD with tape-casting method, the electrocatalytic activity of raw MWCNT CE was much poorer. This also confirms that the electrocatalytic activity of MWCNTs can be enhanced by means of chemical functionalization.

Conclusions

In summary, a simplified process for fabricating MWCNT CEs at low temperature was successfully developed by using chemical functionalization and EPD in this study. Raman, FTIR, SEM, and CV measurements confirmed that the defects and open ends can be obtained on the MWCNT surface via chemical functionalization, thus facilitating the enhancement in the electrocatalytic activity of MWCNTs. In addition, the CV with the consecutive 50 cycles demonstrated that an excellent electrochemical stability of the as-prepared MWCNT CEs can be obtained. In comparison with the tape-casting approach, the MWCNT CE fabricated by EPD presented better adhesion and an electrocatalytic activity due to the shielding effect on MWCNTs by the binder used in paste for doctor blade. Although the cell efficiency of this kind of MWCNT CE was still a little bit low, we believe that MWCNT CE deposited by EPD could be of great potential for use in low-cost DSSCs and open up new avenues for CEs using flexible substrates when the MWCNTs with a larger surface area can be further employed.

Acknowledgments The authors are very grateful to the National Science Council in Taiwan for its financial support under Contract No. NSC-100-2221-E-036-022. We also express our thanks to Dr. Wei in Tripod Technology Corporation for his helpful discussion and partly material support.

References

1. Grätzel M (2001) Nature 414:338–344
2. Lin CY, Lin JY, Lan JL, Wei TC, Wan CC (2010) Electrochem Solid State Lett 13:D77–D79
3. Lin CY, Lin JY, Wan CC, Wei TC (2011) Electrochim Acta 56:1941–1946
4. Kay A, Grätzel M (1996) Sol Energy Mater Sol Cells 44:99–117
5. Suzuki K, Yamamoto M, Kumagai M, Yanagida S (2003) Chem Lett 32:28–29
6. Ramasamy E, Lee WJ, Lee DY, Song JS (2008) Electrochem Commun 10:1087–1089
7. Murakami TN, Ito S, Wang Q, Nazeeruddin MK, Bessho T, Cesar I, Liska P, Humphry-Baker R, Comte P, Pechy P, Grätzel M (2006) J Electrochem Soc 153:A2255–A2261
8. Lee WJ, Ramasamy E, Lee DY, Song JS (2009) Appl Mater Interfaces 1:1145–1149
9. Denaro T, Baglio V, Girolamo M, Antonucci V, Arico AS, Matteucci F, Ornelas R (2009) J Appl Electrochem 39:2173–2179
10. Choi HJ, Shin JE, Lee WG, Park NG, Kim KK, Hong SC (2010) Current Appl Phys 10:S165–S167
11. Nam JG, Park YJ, Kim BS, Lee JS (2010) Scripta Materialia 62:148–150
12. Saito Y, Kubo W, Kitamura T, Wada Y, Yanagida S (2004) J Photochem Photobiol A Chem 164:153–157
13. Chen JG, Wei HY, Ho KC (2007) Sol Energy Mater Sol Cells 91:1472–1477
14. Murakami TN, Grätzel M (2008) Inorg Chim Acta 361:572–580
15. Wu JH, Li QH, Lan Z, Li PJ, Lin JM, Hao SC (2008) J Power Sources 181:172–176
16. Wang M, Anghel AM, Marsan B, Ha NC, Pootrakulchote N, Zakeeruddin SM, Grätzel M (2009) J Am Chem Soc 131:15976–15977
17. Lin JY, Laio JH, Wei TC (2011) Electrochem Solid-State Lett 14: D41–D44
18. Lin JY, Laio JH, Hung ZY (2011) Electrochem Commun 13:977–980
19. Lin JY, Laio JH, Chou SW (2011) Cathodic electrodeposition of highly porous cobalt sulfide counter electrodes for dye-sensitized solar cells. Electrochim Acta. doi:10.1016/j.electacta.2011.07.080
20. Nugent JM, Santhanam KSV, Rubio A, Ajayan PM (2001) Nano Lett 1:87–91
21. Banks CE, Compton RG (2006) Analyst 131:15–21
22. Mei X, Cho SJ, Fan B, Ouyang J (2010) Nanotechnology 21:395202
23. Jhong HR, Wong DS, Wan CC, Wang YY, Wei TC (2009) Electrochem Commun 11:209–211
24. Chiang YC, Lin WH, Chang YC (2011) Appl Sur Sci 257:2401–2410
25. Banks CE, Davies TJ, Wildgoose GG, Compton RG (2005) Chem Commun 7:829–841